

Rare Missense and Synonymous Variants in UBE1 Are Associated with X-Linked Infantile Spinal Muscular Atrophy

Juliane Ramser,¹ Mary Ellen Ahearn,² Claus Lenski,¹ Kemal O. Yariz,² Heide Hellebrand,¹ Michael von Rhein,³ Robin D. Clark,⁴ Rita K. Schmutzler,⁵ Peter Lichtner,⁶ Eric P. Hoffman,⁷ Alfons Meindl,^{1,*} and Lisa Baumbach-Reardon²

X-linked infantile spinal muscular atrophy (XL-SMA) is an X-linked disorder presenting with the clinical features hypotonia, areflexia, and multiple congenital contractures (arthrogryposis) associated with loss of anterior horn cells and infantile death. To identify the XL-SMA disease gene, we performed large-scale mutation analysis in genes located between markers *DXS8080* and *DXS7132* (Xp11.3–Xq11.1). This resulted in detection of three rare novel variants in exon 15 of *UBE1* that segregate with disease: two missense mutations (c.1617 G→T, p.Met539Ile; c.1639 A→G, p.Ser547Gly) present each in one XL-SMA family, and one synonymous C→T substitution (c.1731 C→T, p.Asn577Asn) identified in another three unrelated families. Absence of the missense mutations was demonstrated for 3550 and absence of the synonymous mutation was shown in 7914 control X chromosomes; therefore, these results yielded statistical significant evidence for the association of the synonymous substitution and the two missense mutations with XL-SMA ($p = 2.416 \times 10^{-10}$, $p = 0.001815$). We also demonstrated that the synonymous C→T substitution leads to significant reduction of *UBE1* expression and alters the methylation pattern of exon 15, implying a plausible role of this DNA element in developmental *UBE1* expression in humans. Our observations indicate first that XL-SMA is part of a growing list of neurodegenerative disorders associated with defects in the ubiquitin-proteasome pathway and second that synonymous C→T transitions might have the potential to affect gene expression.

Motor neuron diseases (MND) represent a heterogeneous group of disorders with respect to clinical presentation, disease course, genetic identity, underlying mutations, and etiologies. They are generally characterized by weakness due to muscle atrophy and/or spastic paralysis reflecting the selective involvement of lower and/or upper motor neurons. The most common childhood motor neuron diseases are the autosomal-recessive (AR)-proximal spinal muscular atrophies (AR-SMA) associated with deterioration and destruction of anterior horn cells¹ (MIM #253300, MIM #253550, MIM #253400). These disorders, which are caused by mutations in the *SMN1* gene (MIM #600354, GenBank accession number NM_000344), are often fatal, leading to progressive symmetrical limb and trunk paralysis and severe muscle atrophy. Considerable clinical heterogeneity has been reported.^{2,3} It has long been suggested that a distinct X-linked SMA syndrome exists, similar to Type I SMA (MIM #253300), but associated with congenital contractures (and fractures). This syndrome may be related to arthrogryposis (ARGY), a complex clinical phenotype involving multiple congenital contractures and limited movement of multiple body areas, more often distal than proximal.⁴ Over the last decade, we have come to appreciate a previously unrecognized form of SMA (X-linked infantile spinal muscular atrophy [XL-SMA] [MIM #301830]), which indeed presents with the clinical char-

acteristics of hypotonia, areflexia, and multiple congenital contractures (arthrogryposis) associated with loss of anterior horn cells and death in infancy.⁵ Based on our cumulative experience, we have constructed a list of the defining features and laboratory findings associated with XL-SMA. These can be described as follows: congenital hypotonia; arthrogryposis ± bone fractures; dysmorphic features, including myopathic facies and digital contractures; death of at least one affected within 1 year of birth, due to respiratory distress; family history of miscarriages/spontaneous abortions; genital abnormality (undescended testes); muscle biopsy confirmation of neurogenic atrophy; electromyogram (EMG) indicative of denervation; and autopsy showing anterior horn cell loss. In 1995, we defined a pericentromeric candidate interval for XL-SMA in Xp11.3–Xq11.2 with positive LOD scores between markers *MAOB* and *DXS991*.⁶ Through further analysis of additional XL-SMA families via numerous microsatellite and SNP markers, we recently confirmed and slightly narrowed this linkage interval to an approximately 20.4 Mb region between markers *DXS8080* and *DXS7132* in Xp11.3–Xq11.1.⁵ To identify the underlying disease gene, we now established a gene catalog in the refined interval and performed mutation screening in 123 genes by applying a direct sequencing approach. This approach was carried out on genomic DNA including exons and the adjacent

¹Department of Obstetrics and Gynecology, Technical University Munich, 81675 Munich, Germany; ²Dr. John T. Macdonald Center for Medical Genetics, University of Miami Miller School of Medicine, Miami, FL 33136, USA; ³Department of Neuropediatrics, University Children's Hospital Mainz, 55101 Mainz, Germany; ⁴Department of Pediatrics, Loma Linda University School of Medicine, Loma Linda, CA 92350, USA; ⁵Department of Gynecology and Obstetrics, University of Cologne, 50931 Cologne, Germany; ⁶Institute of Human Genetics, GSF National Research Centre of Environment and Health, 85764 Neuherberg, Germany; ⁷Children's National Medical Center, Research Center for Genetic Medicine, Washington, DC 20010, USA

*Correspondence: alfons.meindl@lrz.tu-muenchen.de

DOI 10.1016/j.ajhg.2007.09.009. ©2008 by The American Society of Human Genetics. All rights reserved.

Table 1. Detected Mutations in Six Screened XL-SMA Families

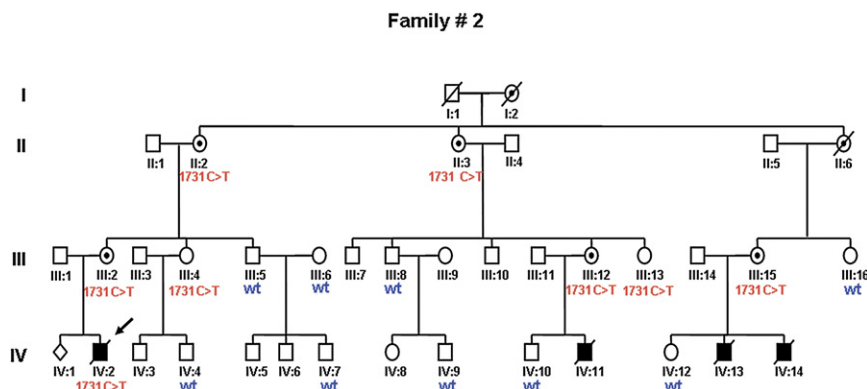
XL-SMA Families	Origin	Detected Mutation	Mutation-Negative X Chromosomes
Family #2	N. American/white	c.1731 C→T p.Asn577Asn	7914
Family #4	N. American/white	c.1731 C→T p.Asn577Asn	7914
Family #5	N. American/white	c.1617 G→T p.Met539Ile	3550
Family #7	N. American/white	c.1639 A→G p.Ser547Gly	3550
Family #9	Mexican	No mutation	-
Family #15	Thai	c.1731 C→T p.Asn577Asn	7914

A total of 3550 control X chromosomes were screened for the three mutations by DHPLC or a direct sequencing approach. Out of these, 3300 X chromosomes were derived from 1650 white females and 250 X chromosomes from healthy white males. DHPLC analysis (WAVE, Transgenomics) was performed under the following conditions: gradient of B buffer, 58%–68%; running temperature, 62°C; forward primer, TAA GTG AGC TTT GTT CCC C; reverse primer, CAG ATG CCT GGC CTC TTT C. Another 4364 X chromosomes were screened for the synonymous C→T substitution by MALDI-TOF mass spectrometer analysis. Out of these, 4350 X chromosomes were derived from 2175 white females and 14 X chromosomes from healthy white males. MALDI-TOF analysis (Sequenom MassArray system) was performed by the homogeneous mass extension (hME) process for producing primer extension products.²¹ Assays were designed with the SpectroDesigner software. Primer sequences are available upon request.

intronic sequences and on cDNA. DNA and RNA were extracted from blood samples, fibroblast cell lines, and immortalized lymphoblastoid cell lines. The screening was performed in a total of six XL-SMA families. All human subject activities occurred in compliance with an active human subject protocol, which has institutional approval. Patient's identification and recruitment are described in detail by Dressman et al. (2007).⁵ In brief, all families were ascertained based on affected males showing diagnostic features described above. Patients meeting study criteria were recruited and consent was obtained by standard procedures. These screening efforts resulted not only in the detection of a number of known polymorphisms in several genes (data not shown), but importantly in the detection of two novel missense mutations (c.1617 G→T, p.Met539Ile; c.1639 A→G, p.Ser547Gly) in two families (families #5 and #7) and a novel synonymous C→T substitution (c.1731 C→T, p.Asn577Asn) in the index patients of another three families (families #2, #4, #15). All aberrations are located in exon 15 of the *UBE1* gene (MIM *314370; GenBank accession numbers NM_003334 and NM_153280) (Table 1, Figures 1 and 2). Sequences of used primer pairs for *UBE1* screening are available on request. Interestingly, the gene is located within a 2.4 Mb interval described as a potential hotspot for neurogenetic disorders.⁷ *UBE1* codes for the

ubiquitin-activating enzyme E1 that catalyzes in the ubiquitin-proteasome system (UPS), the first step in ubiquitin conjugation to mark cellular proteins for degradation.^{8,9} The UPS, as a ubiquitin-dependent proteolysis system, is a fundamental cellular mechanism for regulating protein activity.¹⁰ The three mutations segregate with disease in the families (Figure 1) and were shown by DHPLC analysis (WAVE, Transgenomics) or direct sequencing approaches to be absent in 3550 control X chromosomes (Table 1). Additionally, 4364 control X chromosomes were negatively screened for the synonymous C→T substitution by MALDI-TOF mass spectrometer analysis (Sequenom MassArray system), and therefore a total of 7914 X chromosomes were shown to be negative for this alteration (Table 1). Strictly anonymized DNA of unrelated control individuals was provided by the German Breast Cancer Consortium and the UM/MHRI Cardiovascular Genetics Laboratory in Miami.

With two-sided Fisher's exact tests as implemented in R software (release 2.4.1), these numbers yielded statistical significant evidence for an association of the synonymous substitution and the two missense mutations with XL-SMA (synonymous mutation: $p = 2.416 \times 10^{-10}$, OR = infinite, 95% confidence interval 693.15 to infinite; missense mutations: $p = 0.001815$; OR = infinite, 95 confidence interval

**Figure 1. Pedigree of XL-SMA Family #2**

As described by Kobayashi et al.⁶ Affected males are indicated by black boxes, obligate carriers with a dotted circle. The index patient is marked with an arrow. The synonymous C→T substitution (c.1731 C→T, p.Asn577Asn) was shown by direct sequencing approaches to segregate with disease in the family.

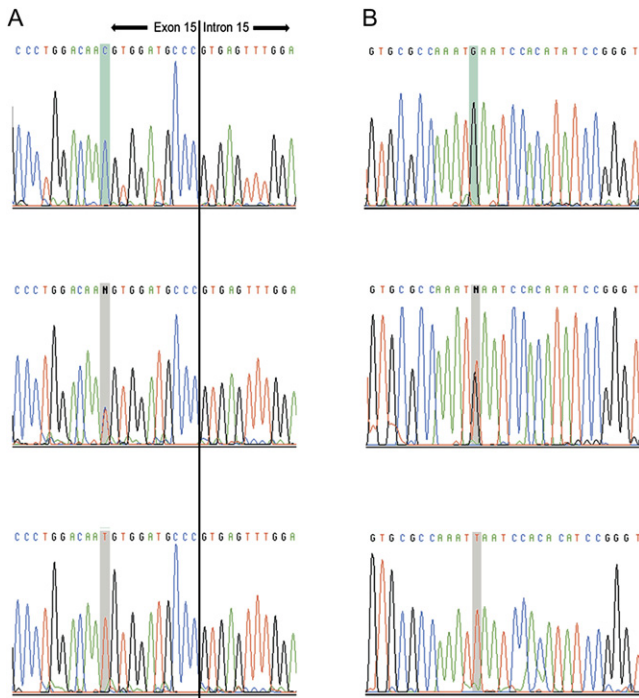


Figure 2. Sequence Alterations Detected in Exon 15 of the *UBE1* Gene

(A) The synonymous c.1731 C→T substitution. Top, wild-type sequence with the “C” highlighted in blue; center, heterozygote status in an obligate carrier; bottom, C→T substitution in a patient with the “T” highlighted in gray.

(B) The c.1617 G→T substitution, p.Met539Ile in family #5. Top, wild-type sequence; center, heterozygote status of an obligate carrier; bottom, G→T substitution in a patient.

14.10 to infinite). Therefore, we postulate mutations in *UBE1* to be the underlying disease causing genetic defects for XL-SMA.

By a systematic analysis of human genetic variations, it was determined recently that up to 70% of low-frequency missense alleles are deleterious, suggesting that the low allele frequency of a rare amino acid variant can, by itself, serve as a predictor of its functional significance.¹¹ Moreover, the two missense mutations detected in families #5 and #7 are located in a part of the transcript that codes for a highly conserved protein domain (Figure 3) that forms interactions with gigaxonin.¹² Allen and colleagues describe gigaxonin as a member of the BTB/kelch superfamily that is important for axonal structure and neuronal maintenance. By building complexes with *UBE1*, gigaxonin controls the degradation of ubiquitin-mediated microtubule-associated protein 1B (MAP1B). Because it interacts with *UBE1*, gigaxonin was suggested to function as a scaffold protein in the ubiquitin-proteasome system (UPS). The authors showed that overexpression of gigaxonin leads to enhanced degradation of MAP1B-LC, whereas overexpression of MAP1B in wild-type cortical neurons leads to cell death.¹² Aberrations of the amino acid sequence in the interaction domain of *UBE1*, as caused by

the two detected missense mutations, may well lead to a disturbed complex building with gigaxonin and as a consequence, to impaired MAP1B degradation. Thus, an increase of MAP1B protein may enhance neuronal cell death with negative consequences also in motoneurons.

In contrast to the two missense mutations, the synonymous C→T substitution detected in families #2, #4, and #15 does not alter the protein sequence, so we first performed quantitative PCR experiments in lymphoblastoid and fibroblastoid cell lines of two index patients, respectively (families #2 and #4) to investigate whether the alteration may influence *UBE1* expression in these cells. These analyses revealed no expression differences in the two patients' cell lines as compared to cell lines from healthy control individuals. The same result was obtained by western blot analysis. Also, no differences in expression were detectable in a cell line of the index patient of family #4 as compared to healthy controls (data not shown). However, as has been reported, *UBE1* displays significant differences in gene expression depending on whether it is analyzed in native tissue or in cell cultures derived from the same biopsies.¹³ Therefore, we performed real-time PCR in white blood cells of the still living index patient of family #15. PCR amplification and detection was performed on a Sequence Detection System (ABI PRISM 7000, Applied Biosystems) applying the standard two-step protocol (45 cycles, annealing temperature 61°C) recommended by ABI. The forward primer (CCC TGG GAT GTC ACG AAG TT) was located at exon boundary 14–15, and the reverse primer (ATG CGG GCA TCC ACG TT) at exon boundary 15–16. The specific probe (FAM-TCC GGG TGA CAA GCC ACC AGA-TMR) was located in exon 15 (TIBMOLBIOL). The genes for 18sRNA and HPRT were used as references (ABI). These analyses revealed a reduction of expression in the patient to one-fifth as compared to blood cells of three healthy controls, thereby implying an impact of the synonymous substitution on gene expression. The consequence of this substitution in the patients might be even more prominent in developing spinal cord, in which *UBE1* was shown to be highly expressed (P. Tsoulfas and P.M. Wood, personal communication).

Although we could not detect any visible alternative splice variants on agarose gels, we could not rule out that the detected reduction of expression of the *UBE1* wild-type transcript was caused by aberrant splicing processes. For this reason, we applied the in silico ESEfinder tool (release 2.0) to determine whether the synonymous C→T exchange may alter existing exonic splicing enhancer motifs or introduce a novel one.¹⁴ This analysis revealed that the exchange leads, in close proximity to another splice enhancer motif “GGACAACG,” to the generation of a second putative exonic splice enhancer motif “TGTGGA.” This new motif could be recognized by the SRp55 protein, which belongs to a family of highly conserved splicing factors that bind to ESEs and are able to promote exon definition.¹⁴ It seems possible that the introduction of an additional splice enhancer motif results in a competitive

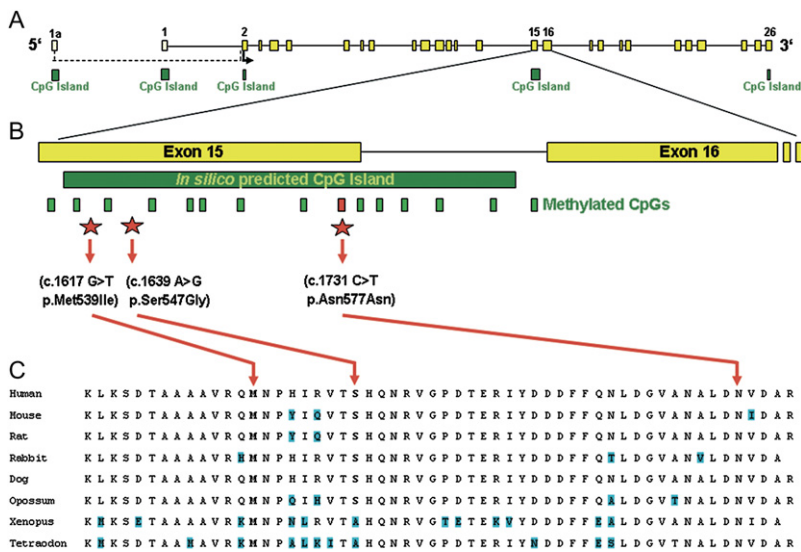


Figure 3. Genomic Structure of the *UBE1* Gene and Amino Acid Conservation of Exon 15 in Several Species

(A) Yellow boxes represent the 26 exons of *UBE1* with an alternative exon 1a. The gene structure was obtained from publicly available databases (UCSC Genome Bioinformatics). Translation start in exon 2 is indicated with a black arrow. Five exonic CpG islands were detected by using *in silico* CpG island prediction tools (MethPrimer).

(B) Position of CpG island and the methylated CpG dinucleotides in exon 15 are represented by green boxes. In index patients of three XL-SMA families, one C methylation less is observed resulting from the C→T exchange (red box). For bisulphite genomic sequencing, genomic DNA was isolated from cell lines or whole blood by means of the DNA Extraction Mini Kit (QIAGEN). The bisulfite modification reaction was performed with the EZ DNA Methylation Kit (HISSE Diagnostics), and the bisul-

phite-treated DNA was amplified with primer pair (1f, 5'-GGT GAA TGT ATA AAT AAG TGA GT-3'; 1r, 5'-ACA CCC CTC TTA ATA TAT ACA C-3') and subsequently sequenced with Big Dye kits (Perkin Elmer). The positions of the three detected mutations in exon 15 are marked with red stars. (C) Exon 15 represents parts of the transcript that codes for a highly conserved protein domain that form interactions with gigaxonin. Amino acid exchanges in the different species are highlighted in blue.

inhibition of the two ESEs and thus alters the splicing process in such a manner that the amount of wild-type transcript becomes reduced in favor of unstable, alternative transcript variants.

We also considered and analyzed an alternative explanation for the observed reduced *UBE1* expression seen in association with the synonymous C→T substitution. As shown in Figure 3, bisulfite genomic sequencing revealed that the substitution involves one CpG dinucleotide out of 13 CpGs that are methylated in healthy controls. These 13 CpGs form a 223 bp large CpG island that is mainly located in exon 15 and partly in intron 15. Because of the C→T exchange, the patients exhibit only 12 methylated cytosins (Figure 3). DNA methylation is described to be essential for normal mammalian embryonic development because it alters the appearance of the major groove of the DNA to which DNA binding proteins can bind.^{15,16} Methylation changes the interactions between these proteins and the DNA, which leads to alterations in chromatin structure and either to a decrease or an increase in the rate of transcription. Whereas methylation of a promoter CpG island leads to the binding of methylated CpG binding proteins and transcription repressors to block transcription initiation, methylation of silencer and so-called insulator elements impede the binding of cognate-binding proteins that potentially abolishes their repressive activities on gene expression.^{16,17} In the case of *UBE1*, one may speculate, that the detected methylated CpG island in exon 15 harbors an element that acts in an insulator-like manner. Although we found the promoter site of *UBE1* to be unmethylated (data not shown), the methylation of this putative element might prevent the binding of specific proteins that act as transcription repressors by blocking specific transcription enhancer elements. In our favored

model (Figure 4), the observed C→T aberration would alter the required methylation pattern at this site, and as a consequence, the specific transcription repressors would bind and possibly block specific transcription enhancers necessary for required *UBE1* expression.

Taken together, the presented data provide strong evidence that the rare missense and synonymous mutations detected in exon 15 of *UBE1* are associated with X-linked spinal muscular atrophy (XL-SMA). We strongly suggest that an alteration of the *UBE1*-mediated ubiquitin-proteasome system results in disturbed neuronal/motor-neuron development, resulting in the XL-SMA disease phenotype.

Ciechanover stated in his Nobel lecture in 2004 about the ubiquitin-proteasome system that "with the multitude of substrates targeted and processes involved, it is not surprisingly that aberrations in the ubiquitin-proteasome pathway have been implicated in the pathogenesis of many diseases, among them certain malignancies and neurodegenerations."¹⁰ A growing list of neurodegenerative disorders has been associated with primary or secondary defects in ubiquitination, primarily in the ubiquitin-proteasome pathway.¹⁸ For example, mutations in Parkin (*PARK2*), an E3 ligase (MIM *602544), or the ubiquitin carboxy-terminal hydrolase L1 (*UCHL1* [MIM +191342]) have been demonstrated in patients with Parkinson's disease (PD), PD [MIM #600116, MIM #168600].¹⁸ Very recently, mutations in the *CUL4B* gene (MIM *300304), encoding an E3 ligase subunit, were found to be causative for an X-linked form of mental retardation associated with neurological features like tremor, seizures, ataxia, and wasting of calf muscles (MIM #300354).¹⁹ To date, pathogenic mutations in human *UBE1* have not been reported and we report here the first ones for this gene, associated with an

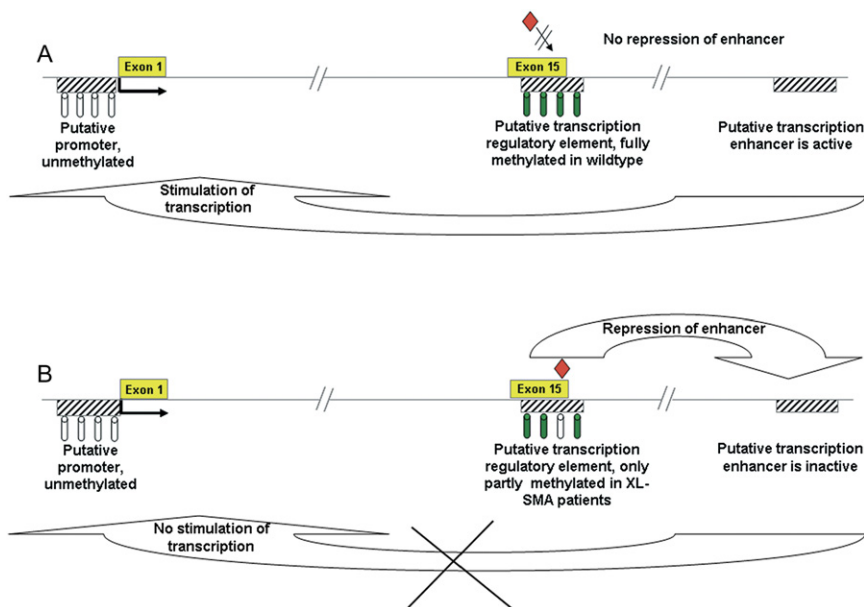


Figure 4. Model for Suggested Transcription Regulatory Element in Exon 15 of *UBE1*

(A) In the wild-type, the CpG island in exon 15 is fully methylated (symbolized by four green cylinders), which prevents the binding of proteins (red diamond) that block a specific transcription enhancer element, thus allowing a putative enhancer to stimulate the transcription.

(B) In the XL-SMA patient harboring the synonymous C→T exchange, the CpG island in exon 15 is only partly methylated (symbolized by a white cylinder among three green cylinders), thus allowing the proteins to bind and as a consequence the transcription enhancer is blocked.

early-onset neurodegenerative disorder involving lower motor neurons. Moreover, the knowledge that SMN, the protein affected in AR-SMA, is also degraded via the ubiquitin-proteasome pathway may well provide important clues into our understanding of common disease mechanisms that produce anterior horn cell death in early childhood, as well as provide hope for design of therapeutic interventions for these biologically related, but genetically distinct, fatal childhood disorders.²⁰

Acknowledgments

The authors are grateful to the numerous clinicians and families that have supported these studies through their cooperation throughout the years. In particular, we would like to acknowledge the contributions of Dr. R. Best and J. Edwards (University of South Carolina Medical Center); R.D.C. and her genetic counselling staff (Loma Linda Medical Center); Drs. D. Rita, C. Booth, and E. Moran (Lutheran General Hospital); Dr. R. Martin (St. Louis University); Dr. K. Flannigan (University of Utah School of Medicine); and Dr. S. Sacharow (Dr. John T. Macdonald Center for Medical Genetics, Miami). We would also like to thank Baylor College of Medicine, Institute of Human Genetics Cell Line facility (J. Belmont, M.D., Director), and the University of Miami Gene Cure Cytogenetics Laboratory (Y.-S. Fan, M.D., Director) for the establishment and maintenance of family cell lines. We would like to thank the German Breast Cancer Consortium for providing DNA samples. We would also like to acknowledge the helpful discussions and information provided by Dr. S. Khuri (Dr. John T. Macdonald Center for Medical Genetics, Miami, FL) and the guidance of Drs. R. Howell, W. Bradley, and L. Elsas throughout the course of these studies. We also thank Dr. B. Mueller-Myhsok for support in statistical analysis and M. Bertone for technical assistance. This work was supported in the United States by funds from the Dr. John T. Macdonald Center for Medical Genetics, University of Miami—Miller School of Medicine and the University of Miami—Miller School of Medicine (to L.B.-R.). The national Muscular Dystrophy Association and the Families of SMA have also provided past support to L.B.-R. and E.P.H. for these investigations. This work was sup-

ported in Europe by the German Ministry for Research and Education grant BMBF 01KW9974 (to A.M.). C.L. was supported by the FAZIT-Stiftung, Frankfurt/Main, Germany.

Received: July 25, 2007

Revised: August 29, 2007

Accepted: September 6, 2007

Published online: January 10, 2008

Web Resources

The URLs for data presented herein are as follows:

ESEfinder, <http://rulai.cshl.edu/tools/ESE2/>
 GenBank, <http://www.ncbi.nlm.nih.gov/Genbank/>
 MethPrimer, <http://www.uogene.org/methprimer/>
 NCBI SNP database, <http://www.ncbi.nlm.nih.gov/SNP/>
 Online Mendelian Inheritance in Man (OMIM), <http://www.ncbi.nlm.nih.gov/OMIM/> (for SMA Type I, II, and III, XL-SMA, *UBE1*, PDJ, PD, *PARK2*, *UCHL1*, and *SMN1*).
 R-Project (language and environment for statistical computing and graphics; release 2.4.1.), <http://www.r-project.org>
 UCSC Genome Bioinformatics, <http://genome.ucsc.edu/>

References

1. Brahe, C., and Bertini, E. (1996). Spinal muscular atrophies: recent insights and impact on molecular diagnosis. *J. Mol. Med.* 74, 555–562.
2. Zerres, K., Wirth, B., and Rudnik-Schoeneborn, S. (1997). Spinal muscular atrophy-clinical and genetic correlations. *Neuromuscul. Disord.* 7, 202–207.
3. Dubowitz, V. (1991). Chaos in classification of the spinal muscular atrophies of childhood. *Neuromuscul. Disord.* 1, 77–80.
4. Banker, B.Q. (1994). Congenital deformities. In *Myology*, A.G. Engel and C. Franzini-Armstrong, eds. (New York: McGraw-Hill), pp. 1905–1933.
5. Dressman, D., Ahearn, M.E., Yariz, K.O., Basterrecha, H., Martinez, F., Palau, F., Barmada, M.M., Clark, R.D., Meindl, A.,

- Wirth, B., et al. (2007). X-linked infantile spinal muscular atrophy: clinical definition and molecular mapping. *Genet. Med.* 9, 52–60.
6. Kobayashi, H., Baumbach, L., Matise, T.C., Schiavi, A., Greenberg, F., and Hoffman, E.P. (1995). A gene for a severe lethal form of X-linked arthrogryposis (X-linked infantile spinal muscular atrophy) maps to human chromosome Xp11.3-q11.2. *Hum. Mol. Genet.* 4, 1213–1216.
 7. Thiselton, D.L., McDowall, J., Brandau, O., Ramser, J., d'Esposito, F., Bhattacharya, S.S., Ross, M.T., Hardcastle, A.J., and Meindl, A. (2002). An integrated, functionally annotated gene map of the DXS8026–ELK1 interval on human Xp11.3–Xp11.23: potential hotspot for neurogenetic disorders. *Genomics* 79, 560–572.
 8. Tanaka, K., Suzuki, T., Hattori, N., and Mizuno, Y. (2004). Ubiquitin, proteasome and parkin. *Biochim. Biophys. Acta* 1695, 226–238.
 9. Rubinsztein, D.C. (2006). The roles of intracellular protein-degradation pathways in neurodegeneration. *Nature* 443, 780–787.
 10. Ciechanover, A. (2005). Intracellular protein degradation: from a vague idea thru the lysosome and the ubiquitin-proteasome system and onto human diseases and drug targeting. Review: Nobel Lecture. *Cell Death Differ.* 12, 1178–1190.
 11. Kryukov, G.V., Pennacchio, L.A., and Sunyaev, S.R. (2007). Most rare missense alleles are deleterious in humans: implications for complex disease and association studies. *Am. J. Hum. Genet.* 80, 727–739.
 12. Allen, E., Ding, J., Wang, W., Pramanik, S., Chou, J., Yau, V., and Yang, Y. (2005). Gigaxonin-controlled degradation of MAP1B light chain is critical to neuronal survival. *Nature* 438, 224–228.
 13. Nino-Soto, M.I., Nuber, U.A., Basrur, P.K., Ropers, H.H., and King, W.A. (2005). Differences in the pattern of X-linked gene expression between fetal bovine muscle and fibroblast cultures derived from the same muscle biopsies. *Cytogenet. Genome Res.* 111, 57–64.
 14. Cartegni, L., Wang, J., Zhu, Z., Zhang, M.Q., and Krainer, A.R. (2003). ESEfinder: a web resource to identify exonic splicing enhancers. *Nucleic Acids Res.* 31, 3568–3571.
 15. Okano, M., Bell, D.W., Haber, D.A., and Li, E. (1999). DNA Methyltransferases Dnmt3a and Dnmt3b are essential for de novo methylation and mammalian development. *Cell* 99, 247–257.
 16. Jones, P.A., and Takai, D. (2001). The role of methylation in mammalian epigenetics. *Science* 293, 1068–1070.
 17. Bell, A.C., West, A.G., and Felsenfeld, G. (1999). The protein CTCF is required for the enhancer blocking activity of vertebrate insulators. *Cell* 98, 387–396.
 18. Ross, C.A., and Pickart, C.M. (2004). The ubiquitin-proteasome pathway in Parkinson's disease and other neurodegenerative diseases. *Trends Cell Biol.* 14, 703–711.
 19. Tarpey, P.S., Raymond, F.L., O'Meara, S., Edkins, S., Teague, J., Butler, A., Dicks, E., Stevens, C., Tofts, C., Avis, T., et al. (2007). Mutations in CUL4B, which encodes a ubiquitin E3 ligase subunit, cause an X-linked mental retardation syndrome associated with aggressive outbursts, seizures, relative macrocephaly, central obesity, hypogonadism, pes cavus, and tremor. *Am. J. Hum. Genet.* 80, 345–352.
 20. Chang, H.C., Hung, W.C., Chuang, Y.J., and Jong, Y.J. (2004). Degradation of survival motor neuron (SMN) protein is mediated via the ubiquitin/protease pathway. *Neurochem. Int.* 45, 1107–1112.
 21. Tang, K., Fu, D.J., Julien, D., Braun, A., Cantor, C.R., and Koster, H. (1999). Chip-based genotyping by mass spectrometry. *Proc. Natl. Acad. Sci. USA* 96, 10016–10020.